Ir ernational Journal of Ocean Engineering and Technology Vol. 5, No. 1, pp 29~39, December 2002 (ISSN 1229-1668)

# Wave Boundary Layer: Parameterization Technique and Its Proof

M. BELEVICH*, A. SAFRAY*, KWI-JOO LEE** AND KYOUNG-HWA KIM**
*Wave Research Center, General Physics Institute, Russian Academy of Sciences, Russia
**Department of Naval Architecture and Ocean Engineering, Chosun University, Gwangju, Korea
(Received 24 December 2001, accepted 1 February 2002)

**ABSTRACT**: A general investifation into the physical mechanism that is respinsible for drag above the sea surface has been undertaken. On the basis of a 1D model of the Wave Boundary Layer(WBL), under a 2D wave field, a parameterization technique for estimation of the drag and mean characteristics of WBL is described. Special attention is paid to estimation of the simplifying assumption of the theory.

**KEY WORDS**: Wave Boundary Principle, Arbitrary Wind Direction, Parameterization of Drag

## 1. Introduction

The local thermodynamic interaction is an important element of an ocean-atmosphere system. The accuracy of its parameterization determines the quality of climate modeling, weather prediction, and ecological forecasting.

The main problem with the theory of the near-surface boundary layer is the establishment of a relationship between turbulent stress $T$ and wind velocity vector $u$ at an arbitrary

$$T=\rho_a C|u|u \qquad (1)$$

height where $\rho_a$ is air mass density, and $C$ is the drag coefficient. Contrary to the case of the solid lower boundary, which is described by only one morphological characteristic, the roughness parameter $z_0$, the sea surface is not predetermined, due to waves that are produced by local wind and swell.

Far from the surface, at heights more than a wave boundary layer specific height $h_W$, the wave-induced fluctuations attenuate, and in the case of stationary and horizontal, homogeneity the boundary layer above the waves is very close to that which is above a solid flat surface. In particular, the turbulent momentum flux is constant with height and the wind profile is nearly logarithmic.

However, near the waves, the role of wave-induced fluctuations increases, and immediately above the surface, the resemblance to the usual boundary layer completely disappears. The drag coefficient isformed, jointly, by all drag mechanisms arising in the relatively thin layer near the interface.

Existing computational methods for the momentum flux above waves are usually based on simple Charnock's relation $z_0=m\frac{v_*^2}{g}$, where $v_*$ is the friction velocity, $m$ is an empirical coefficient, and $g$ is the gravity acceleration. Although this expression provides a good scale for the roughness parameter, it may be considered as a qualitative estimate, since it does not take into account the specific character of a given wave field. Using Charnock's relation, the drag law may be written as follows

$$\ln\frac{|u|^2}{gz}=-\ln(mC)-\frac{k}{\sqrt{C}} \qquad (2)$$

which connects the drag coefficient $C$ with the wind velocity at any height $z$. Chalikov and Belevich (1993) note that this expression gives a rather weak dependence of $C$ on wind velocity, since it is assumed that the wind and waves are adapted to each other and that the wave field is fully developed. Often, this is not correct, because the space and time scales of a stationary wave field, under a sufficiently strong wind, are too large. As a result, in a general case, the drag coefficient depends not only on the wind velocity, but also on the 2D wave spectrum $S(Vk)$

$$C=C\left(\frac{|u^2|}{gz},S(Vk)\right) \qquad (3)$$

This problem has been considered by Chalikov and Belevich (1993). Using the 1D model of the boundary layer above waves, an approximate formula, which binds the drag

---

The first author : Kwi-Joo Lee
Email : kjalee@chosun.ac.kr

$C$ with wind velocity and wave age, has been developed. However, some simplifying assumptions have been made. They are as follows:

- Angular wave distribution is considered to be symmetric with respect to the wind direction.
- Non-linear inter-mode interactions are regarded as insignificant and are neglected.
- Stratification is assumed to be neutral.

In recent research by Belevich (1996 and 2000) it has been shown that the last two assumptions are quite possible and, in regular meteorological situations, do not generate serious errors. The first assumption has not yet been analyzed. We present such an analysis, here, and summarize all the work done in connection with the problem of parameterization of the wave boundary layer. This is the objective of our study.

The paper is organized as follows. In Section 2, a 1D model of WBL is introduced. Section 3 is devoted to describing parameterization of drag, under a 2D wave field. Estimation of the simplifying assumptions of the model is presented in Section 4.

## 2. 1D Model of the Wave Boundary Layer

Surface wind waves generate a specific wave boundary layer (WBL), whose properties differ from those of the surface mixed layer. The main difference between the WBL and the boundary layer, over a fixed flat surface, is the onset of an additional momentum flux, due to wave fluctuations of pressure, velocity, and turbulent stress. Since the momentum balance takes place in a stationary WBL, the wave-induced momentum flux causes variations of the turbulent momentum flux and deviations in the wind velocity profile from the logarithmic one inside the WBL and additive changes of wind velocity outside the WBL. Within the logarithmic interval of the wind profile, it is convenient to describe these effects using the so-called total roughness parameter, which takes into account the wave drag of both parts of the wave spectrum, i.e. low-frequency part and the universal range, where Phillips' law is assumed. One of the main objectives of this work is elaboration of a computational algorithm for the WBL structure above an arbitrary wave field, including waves produced by non-local wind, i.e. swell.

The structure of the stationary WBL is governed by the momentum balance equation

$$\partial_\zeta(T+\tau)=0 \tag{4}$$

where $T$ and $\tau$ are the vertical components of the turbulent stress and the wave induced stress (or wave induced momentum flux), respectively, $\zeta$ is the vertical coordinate, the origin of which is located on the wave surface.

Assuming that $T=K\partial_\zeta u$, where $K$ is the turbulent viscosity coefficient and u is the horizontal wind velocity, we obtain

$$\partial_\zeta(K\partial_\zeta u+\tau)=0 \tag{5}$$

The upper boundary of the WBL is defined by conditions

$$T\mid_{hw}=T_h,\quad \tau\mid_{h_w}=0 \tag{6}$$

Integration of (5) within $(\zeta, h_W)$, gives

$$K\partial_{\zeta u}+\tau=T_h \tag{7}$$

The unknown coefficient $K$ in equation (7) may be expressed in terms of turbulent energy density $e$ and the so-called mixing length $\ell$

$$K=\ell\sqrt{\frac{e}{c_1}} \tag{8}$$

Here $c_1\approx 4.6$ is an empirical constant. To calculate the scale $\ell$ the simplest hypothesis is used $\ell\approx\varkappa\zeta$. The turbulent energy density $e$ is computed, using the turbulent energy balance equation

$$P+\partial_\zeta K\partial_\zeta e-\frac{1}{\ell}\left(\frac{e}{c_1}\right)^{\frac{3}{2}}=0 \tag{9}$$

The second and third terms describe the diffusion and dissipation of $e$, respectively. The first term is the production of the turbulent energy, via the velocity shift and may be taken in the form (see discussion in Chalikov(1993))

$$P=(K\partial_\zeta u+\tau)\partial_\zeta u=T_h\partial_\zeta u \tag{10}$$

The equation (9) now takes the form

$$T_h d_\zeta u+d_\zeta K d_\zeta e-\frac{1}{\ell}\left(\frac{e}{c_1}\right)^{\frac{3}{2}}=0 \tag{11}$$

Using the scales $v_*^2/g$ for length and $v_*^2/g$ for time, where $v_*$ is treated as $\sqrt{|T_h|/\rho_a}$ we rewrite the system of equations (7), (11) in non-dimensional form (non-dimensional variables are marked by the tilde)

$$\tilde{K} d_{\tilde{\zeta}} \tilde{u} = 1 - \tilde{\tau} \qquad (12)$$

$$d_{\tilde{\zeta}} u + d_{\tilde{\zeta}} \tilde{K} d_{\tilde{\zeta}} \tilde{e} - \frac{1}{\tilde{K}} \left( \frac{\tilde{e}}{c_1} \right)^2 = 0 \qquad (13)$$

The boundary conditions are as follows:

$$\tilde{e} = c_1, \qquad \tilde{\zeta} = \tilde{h}_W \qquad (14)$$

$$d_{\tilde{\zeta}} \tilde{e} = 0, \qquad \tilde{\zeta} = 0 \qquad (15)$$

$$\tilde{K} d_{\tilde{\zeta}} \tilde{u} = C_r | \tilde{u}_r | \tilde{u}_r, \qquad \tilde{\zeta} = \tilde{\zeta}_r \qquad (16)$$

Here $\tilde{u}_r$ and $C_r$ are the wind velocity and the local drag coefficient at the height $\tilde{\zeta}_r$, respectively, and $\tilde{\zeta}_r$ is small enough height lying in the interval $\left( \frac{2\pi}{\tilde{\omega}_2^2}, \frac{2\pi}{\tilde{\omega}_1^2} \right)$, where ($\tilde{\omega}_1$, $\tilde{\omega}_2$) is the fre- quency band which includes Phillips' spectrum

$$\tilde{S}(\tilde{\omega}) = \alpha \tilde{\omega}^{-5}, \qquad \alpha = const \qquad (17)$$

The first boundary condition implies that $\tilde{e}$ is constant, above the wave boundary layer. The second one indicates that at a small height $\tilde{\zeta} = \tilde{\zeta}_r$, dissipation of $\tilde{e}$ is balanced by its production. The necessity to choose a lower boundary condition at height $\tilde{\zeta}_r$ is discussed, in detail, in Chalikov (1993).

Vertical component of the wave-induced momentum flux $\tau$ is computed using the technique suggested in Chalikov (1993). Neglecting the non-linear effects, it is possible to write the flux $\tau$ over an arbitrary wave field as a superposition of the "elementary" wave fluxes $F(\omega)$, which are induced independently by each spectral component:

$$\tau(\zeta) = \rho_w g \int_0^{\omega_r} F(\omega) f(\zeta) d\omega \qquad (18)$$

where $\rho_w$ is the water mass density, $\omega_r$ is the frequency that corresponds to the wavelength $\zeta_r$, and $f(\zeta)$ is the vertical distribution function. The results of numerical experiments with 2D WBL model Makin(1996) allowed suggestions of the approximate formula for the vertical distribution of the momentum flux $\tau$ induced by the mono-chromatic wave Chalikov(1993):

$$f(\zeta) \equiv \frac{\tau}{\tau_0} = \left( 1 - \frac{\xi}{\xi_0} \right) \cdot e^{-10\xi}$$

$$\xi = \frac{\zeta}{\lambda} \qquad \xi_0 = 0.31 - 50 C_\lambda \qquad (19)$$

where $\tau_0$ is the surface value of the momentum flux, $\lambda = \frac{2\pi g}{\omega^2}$ is the wave length, and $C_\lambda$ is the value of drag co- efficient on the height $\zeta = \lambda$. Thus, the disturbances induced by the wave decreases in $e$ times on the height $\zeta$ of the order of $0.1\lambda$. Since the presence of a strongly pronounced maximum on the peak frequency $\omega_p$ and sharp decay in the neighboring low frequency domain are typical features of the developing waves, it is quite natural to define the height of the WBL as the value that is proportional to the wave length of the peak frequency, namely:

$$h_W \approx 0.1 \frac{2\pi g}{\omega_p^2} \qquad (20)$$

The flux $F(\omega)$, which corresponds to the 2D wave spectrum $S(k) = S(\omega) D(\omega, \theta)$, where $S(\omega)$ is the frequency spectrum and $D(\omega, \theta)$ is the angular distribution of the wave field, may be written as follows:

$$F(\omega) = \int_{-\pi}^{\pi} k S(\omega) D(\omega, \theta) \beta(\omega, \theta) d\theta \qquad (21)$$

Here $k = (k_1, k_2)$ is the wave number, $k_1 = \frac{\omega^2}{g} \cos\theta$, $k_2 = \frac{\omega^2}{g} \sin\theta$, and the weight function $\beta$ is the so-called wind-wave interaction (WWI) parameter. The waveward energy flux $\varepsilon$ then reads

$$\varepsilon(\omega) = \rho_w \int_{-\pi}^{\pi} \omega S(\omega) D(\omega, \theta) \beta(\omega, \theta) d\theta \qquad (22)$$

## 3. Parameterization of Drag over the 2D Wave Field

The 1D model, formulated above, has been used to elaborate the parameterization scheme of the WBL over an arbitrary 2D wave field. As an example, two model spectra have been considered: The Pierson-Moscivitz spectrum for developed waves (Hasselmann et al, 1988) and the JONSWAP spectrum approximation for developing sea waves. Below, both spectra are written in terms of relative frequency $o=\frac{\omega}{\omega_p}$.

Pierson-Moskovitz spectrum:

$$S_{PM}(\tilde{\omega})=(\alpha_{PM}\,\tilde{\omega}_p)o^{-5}\exp\left(-\frac{5}{4}o^{-4}\right) \tag{23}$$

where

$$\alpha_{PM}=0.0081,\qquad \tilde{\omega}_{PM}=0.033 \tag{24}$$

JONSWAP spectrum:

$$S_J(\tilde{\omega})=(\alpha_J\,\tilde{\omega}_p)o^{-5}\exp\left(-\frac{5}{4}o^{-4}\right)\gamma_J^{G_J} \tag{25}$$

where

$$\alpha_J=0.57\,\tilde{\omega}_p^{1.5},\qquad \gamma_J=3.3 \tag{26}$$

$$G_J=\exp\left(-\frac{1}{2}\left(\frac{1-o}{\sigma_J}\right)^2\right)$$

$$\sigma_J=\begin{cases}0.07, & o\le 1,\\ 0.09, & o\ge 1.\end{cases} \tag{27}$$

The directional distribution for both spectra was taken in JONSWAP form:

$$D(\tilde{\omega},\theta)=N_s^{-1}\cos^{2s}\left(\frac{\theta}{2}\right) \tag{28}$$

where

$$N_s=\int_{-\pi}^{\pi}\cos^{2s}\left(\frac{\theta}{2}\right)d\theta=2\sqrt{\pi}\frac{\Gamma(s+\frac{1}{2})}{\Gamma(s+1)} \tag{29}$$

$$s=9.77o^{\mu},\qquad \mu=\begin{cases}4.06, & o\le 1,\\ -2.34, & o>1.\end{cases} \tag{30}$$

Here $\Gamma(s)$ is a gamma-function.

Assuming the symmetric angular distribution $D(\tilde{\omega},\theta)$ with respect to wind direction, we let the lateral stress component be equal to zero. Numerical integration of the model equations has been performed for a number of fetches, defined by non-dimensional peak frequency $\tilde{\omega}_p$. The following values of $\tilde{\omega}_p$ were used: 0.06, 0.10, 0.15, 0.20. The Pierson-Moscovitz and JONSWAP spectra for different values of $\tilde{\omega}_p$ are shown in Fig. 1a. The specific feature of this model spectrum is a well- pronounced overshoot effect. That is, for any given frequency $\tilde{\omega} > \tilde{\omega}_p$ the smaller the fetch, the greater the value of the spectral energy density $S_J(\tilde{\omega})$. Fig. 1b shows the spectral density distribution of the energy flux, computed according to Equation (22). The density of the energy flux increases with increasing fetch, and its maximum is located in the vicinity of the peak frequency. The spectral density of the momentum flux (see Fig. 1c) computed according to Equation (21), shows an inverse regularity: its maximum decreases with increasing fetch, due, mainly, to the overshoot effect.

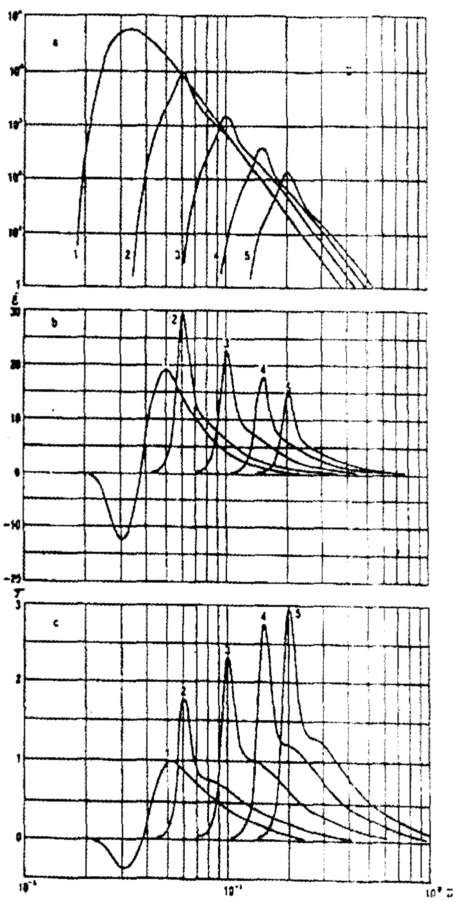

**Fig. 1** (a) Wave spectra $\tilde{S}(\tilde{\omega})$; (b)Wave energy flus density $\tilde{\varepsilon}(\tilde{\omega})$ ; (c) Wave momentum flus density for different wave ages: $1-\tilde{\omega}_P=0.033$ (Pierson-Moscovitz spectrum) $2-\tilde{\omega}_P=0.06$, $3-\tilde{\omega}_P=0.10$, $4-\tilde{\omega}_P=0.15$, $5-\tilde{\omega}_P=0.20$ (JONSWAP spectrum)

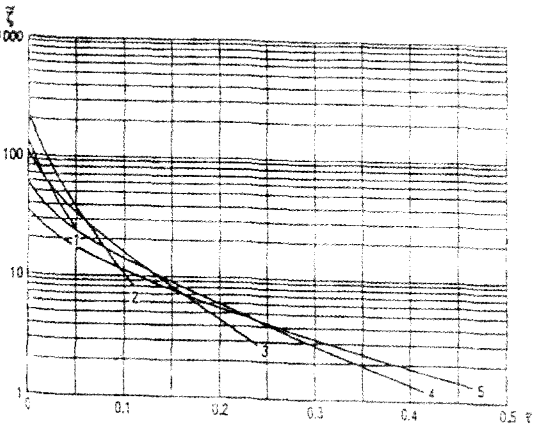


Fig. 2 Vertical distribution of momentum flux $\tau$ for different wave ages. Captions as in Fig. 1

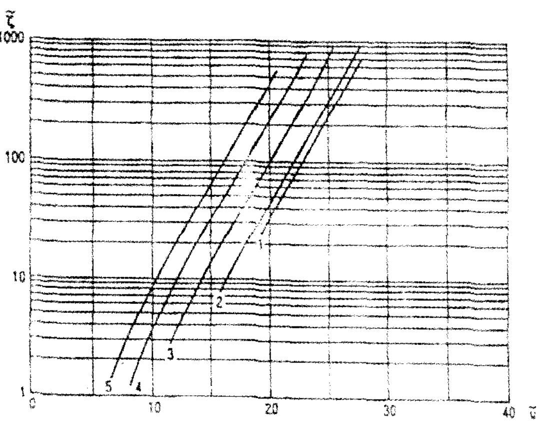


Fig. 3 Vertical profiles of wind velocity $|\tilde{u}|$ for different wave ages. Captions as in Fig. 1

The vertical profiles of the wave-produced momentum flux, computed using (18), are shown in Fig. 2. The larger the fetch, the smaller the flux, but the greater the height, because it is produced by longer waves. In spite of the rapid vertical attenuation of the wave-induced flux of momentum with small fetches, the drag effects are stronger than with large fetches. This phenomenon may be explained using the simplified equation of turbulent energy balance. Neglecting the diffusion, it is possible to obtain the solution

$$\tilde{u} \equiv \frac{1}{\sqrt{C}} = \frac{1}{\varkappa} \int_{\zeta_0}^{\zeta} \frac{(1-\tilde{\tau})^{\frac{3}{1}}}{\zeta} d\zeta \qquad (31)$$

Showing that the drag coefficient depends, monotonically, on the integral of the wave-induced momentum with respect

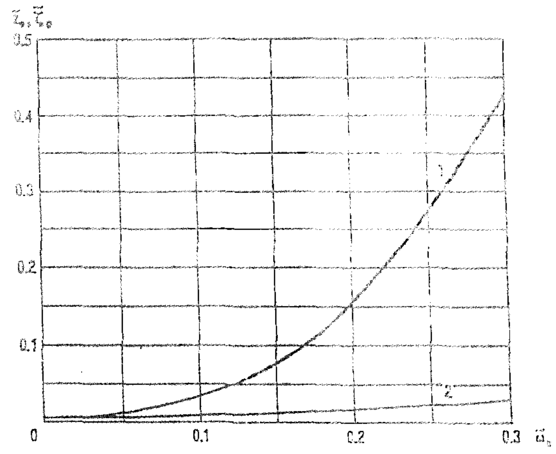


Fig. 4 Dependence of roughness on peak frequency $\tilde{\omega}_p$ : 1- total roughness parameter $\tilde{z}_0$(numerical solution). 2- local roughness parameter $\tilde{\zeta}_0$ in accordance with(33)

to height.

Although $\tilde{\tau}$, at small heights, may be sufficiently large, the wind profiles (Fig. 3) are nearly logarithmic and shifted, due to variations of the total roughness parameter. Thus, except for a thin layer in the vicinity of the wave surface, the following expression,

$$\tilde{z}_0 = \tilde{z}_* e^{\varkappa u} \qquad (32)$$

provides, in practice, the same values of the total roughness parameter.

The dependence of $\tilde{z}_0$ and $\tilde{\zeta}_0$ on $\tilde{\omega}_p$ is shown in Fig. 4. The values of $\tilde{\zeta}_0$ have been calculated using the formula (see (Chalikov and Belevich, 1993))

$$\tilde{\zeta}_0 = 0.075\ \tilde{\omega}_p^{\frac{3}{4}} \qquad (33)$$

Significant variations of $\tilde{\zeta}_0$ with respect to peak frequency (or wave age), demonstrate the important role of the wave-induced drag.

The relation of the drag law type

$$C = C\left(\frac{u^2}{g\zeta}, \tilde{\omega}_p\right) \qquad (34)$$

is a convenient characteristic of the wave boundary layer. This function was calculated using the solution of problem (13)-(16), and is shown in Fig. 5b. Relation (2),

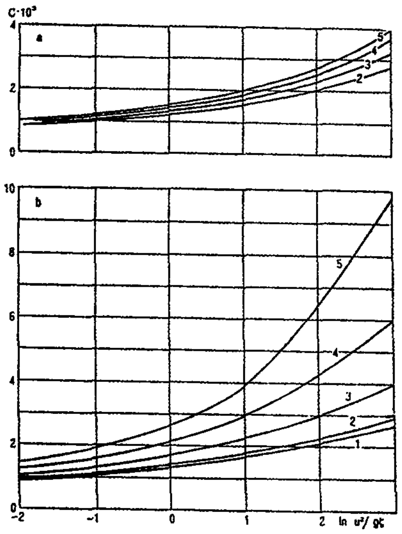


**Fig. 5** Dependence of drag coefficient $C(z)$ on $\ln(|u(z)|^2/gz)$ : (a) $\zeta_0$ depends on $\widetilde{\omega}_p$ only; (b) numerical solution. Captions as in Fig. 1

with non-dimensional local roughness parameter $m$ equal to $\zeta_0$, is plotted in Fig. 5a for comparison. This formula provides a weaker dependence of $C$ on both arguments. Hence, the drag over the sea surface is formed by the specific wave situation, rather than the high-frequency universal part of the spectrum.

Using data in Fig. 5b, it is possible to derive a drag law that connects the drag coefficient at any arbitrary height $\zeta$ with external parameters $R=\ln(u^2/g\zeta)$ and $\Omega=u/c_p$ (where $u$ is the wind velocity at height $\zeta$). This dependence may be approximated by the following relation:

$$\begin{aligned}\ln C = & -6.460+0.102\Omega+0.009\Omega^2 \\ & +(0.311+0.055\Omega+0.006\Omega^2)R \\ & +(0.032+0.011\Omega+0.001\Omega^2)R^2\end{aligned}$$

## 4. Study of the Simplifying Assumptions

The parameterization described, herein has been developed using some simplifying assumptions, namely:

1. Stratification has been assumed to be neutral,
2. Non-linear inter-mode interactions have been regarded as insifnificant, and thus neglected.
3. Angular wave distribution has been considered to be symmetric with respect to the wind direction.

We have considered the possibility of these assumptions, and below, the corresponding results are summarized.

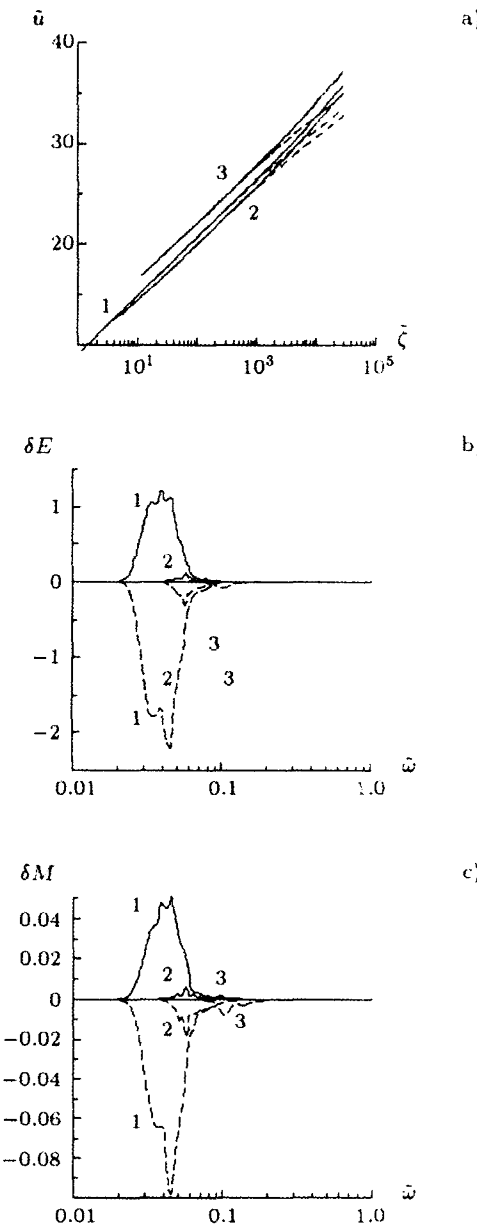


**Fig. 6** Influence of air stratification on the WBL characteristics: (a) wind velocity; (b)deviation of the wave energy flus density $\delta\varepsilon(\widetilde{w})$; (c) wave momentum flus density $\delta F(\widetilde{w})$with respect to the neutral stratification for different wave ages : $1-\widetilde{\omega}_P=0.033$(Pierson-Moscovitz spectrum), $2-\widetilde{\omega}_P=0.06$, $3-\widetilde{\omega}_P=0.10$, , (JONSWAP spectrum). Solid line - $\widetilde{T}_*=0.5\cdot10^{-3}$ , dash line - $\widetilde{T}_*=-1.0\cdot10^{-3}$

### 4.1 Arbitrary Stratification of WBL

The overwhelming majority of investigations, concerning the boundary layer above waves, assume the air within the WBL to be neutrally stratified. To what extent is this assumption limiting? Qualitative, as well as quantitative, estimates have been produced in Belevich (1996).

Wind profiles in a stratified boundary layer differ from the logarithmic profile, and the following (Monin and Yaglom, 1971) may be described using the universal function $\psi$ of the non- dimensional argument $\sigma$:

$$u=\frac{v_*}{x}(\psi(\sigma)-\psi(\sigma_0))$$

$$\sigma=\frac{z}{L_*},\quad \sigma_0=\frac{z_0}{L_*}$$

where $v_*$ is friction velocity, $x=0.4$ is von Karman's constant and $L_*$ is the so- called Monin-Obukhov length scale.

$$L_*=-\frac{v_*^3 c_p\ \rho_a}{xbq}$$

Here $b=g/\overline{T}$ is the buoyancy parameter, $\overline{T}$ is the air mean temperature, $q$ is the turbulent heat flux, and $c_p$ is the heat capacity of the air. Absolute value and sign of $\sigma$ characterize the hydrostatic stability of the medium: the stratification is stable when $\sigma>0$; neutral when $\sigma=0$, and unstable when $\sigma<0$. There are a number of approximate formulas for the function $\psi$, which differ from each other, mainly by values of the constants. The formula that has been derived in Zilitinkenvich and Chalikov (1968), was used in the current research:

$$\psi(\sigma)=\begin{cases}\ln\sigma+10\cdot\sigma, & \sigma>0\\ \ln|\sigma|, & \sigma\in[-0.07,0]\\ 0.25+1.2\sigma^{-\frac{1}{3}}, & \sigma<-0.07\end{cases}$$

This function is close to logarithmic for small values of $\sigma$, and differs from the latter either for large values of $|L_*|$ (heavily stratified medium) or for large heights $z$.

The ratio of the WBL height $h_W$ to the length scale $L_*$ characterizes the influence of thermal stratification on the WBL structure. In the case that the stratification is not too far from the neutral ( $L_*\not\in[-10^2\cdot 10^2]$ ) , the order of magnitude of this ratio is near 0.1, even for developed sea. Therefore, we may expect that the influence of stratification is insignificant for small fetches, increases with developing waves, and becomes apparent, mainly in the low-frequency portion of the spectrum.

The quantitative estimates may be obtained using a modified 1D WBL model. The modification is involved in taking into account mutual transformations of turbulent and potential energies of the liquid column, with variable mass density in the gravity field

$$b\frac{q}{c_p\rho_a}=-\frac{v_*^3}{xL_*}=-xv_*bT_*$$

where $T_*$ is temperature scale which is connected with the length scale $L_*$ via the relation

$$L_*T_*=\frac{v_*^2}{x^{2b}}$$

Using the modification described, the turbulent energy balance equation (13) is now written as follows:

$$d_\zeta u+d_\zeta \tilde{K}d_\zeta \tilde{e}-\frac{1}{\tilde{K}}\left(\frac{\tilde{e}}{c_1}\right)^2-x\ \tilde{T}_*=0$$

where $\tilde{T}_*=T_*/\overline{T}$, $\tilde{T}_*=(x^2\ \tilde{L}_*)^{-1}$, $\tilde{L}_*=gL_*/v_*^2$.

This new problem has been solved for various wave situations and for the values of $\tilde{T}_*$ within the range $[-10^{-3},10^{-3}]$. The developed sea has been simulated, via the Pierson-Moscovitz spectrum (23); in the case of developing seas, the JONSWAP spectrum (25), with $\tilde{\omega}_p=0.06;0.1$, has been used.

The calculations completed verify the above-made qualitative considerations. Wind profiles for non-neutral stratifications (see Fig. 6a) coincide with the logarithmic profile for small heights, and noticeably differ from it near the upper border of the computational domain. The stratification significantly influences the energy and momentum exchange (see Fig. 6b and 6c, respectively) in the case of a developed sea, only when the main energy-bearing part of the spectrum is located in the low-frequency domain. In all other cases, the influence of stratification is negligible. Thus, not taking into account the heavily stratified air of the wave boundary layer over developing waves may be considered, in a first approximation, neutrally stratified, and the above-produced parameteriza -tion scheme may be used without modification.

It is worth mentioning that the results obtained may be used in a more general situation of the mass density stratification. In this case, the scales $L_*$ and $T_*$ should be changed to $L^*$ and $T^*$, respectively:

$$L^*=L_*\left(1+\frac{0.075}{\text{Bo}}\right)^{-1},\quad T^*=T_*\left(1+\frac{0.075}{\text{Bo}}\right) \tag{35}$$

where Bo is the Bowen ratio. For small values of Bo, the influence of the humidity stratification becomes comparable to the effects of the thermal stratification. In this case, the non-dimensional correction term in (35) is close to unity, and must not be neglected.

### 4.2 Superposition Principle

In Belevich and Neelov (2000), the mutual influence of the wave components on the energy interchange with the wave boundary layer has been estimated. In case this influence is negligible, the superposition principle, which plays an important role in the whole theory, is applicable.

The 1D model of the wave boundary layer, described above, has been used in a study of the airflow over a two-mode wave surface. The Low Frequency (LF) mode $\tilde{\omega}_L$ changed within the interval (0.06, 0.4). The values of the High Frequency (HF) mode $\tilde{\omega}_H$ were calculated using the dispersion relation for high frequency wave number $k_H$ divisible by low frequency wave number $k_L$ with the factor equal to $2^n$, $n=1,\cdots,5$. Amplitudes a of the wave modes have been chosen, using the condition $ak=0.1$. Note that according to Makin (1983), as well as our calculations, the dependence of the wind-wave interaction on the wave steepness $ak$ for the values within the range [0.05, 0.3] is nearly absent.

Evaluation of mutual influence of the wave components on the energy interchange with the WBL has been carried out in terms of the wind-wave interaction parameter $\beta(\omega)$. Values of the function $\beta$, calculated for the two-mode surface, have been compared with those of this function $\beta_0$ for single-mode surface. All numerical experiments that were undertaken for various values of the wave parameters, using the 3D model of the WBL (Belevich and Neelov, 1998), demonstrate weak mutual influence on the energy exchange. Values of the function $\beta_H=\beta(\omega_H)$ coincide with those of $\beta_0$(see Fig. 7a). Differences $\Delta\beta_H=\beta_H-\beta_0$ are insignificant for all frequencies (see Fig. 7b). Relative variations of the WWI parameter $\delta\beta_H=\Delta\beta_H/\beta_0$ oscillate within the $\pm 30\%$ limits for low frequencies (i.e. for small values of $\beta$) and decrease with increasing $\omega_H$.

The influence of the HF mode on the energy exchange of the LF wave component is also weak. Fig. 8a shows that the dependence of $\beta_L=\beta(\omega_L)$ on the frequency of the HF oscillation noticeably differs from the constant for small values of $\omega_L$ only, i.e. when $|\beta|$ is small. The calculated differences $\Delta\beta_L=\beta_L-\beta_0$ demonstrate that the presence of the HF mode manifests itself in an insignificant decrease of the parameter $\beta_L$ (see Fig. 8b). However, the relative decrease of the WWI parameter $\delta\beta_L=\Delta\beta_L/\beta_0$ do not exceed 5%.

Though the results obtained indicate the existence of mutual influence of the wave components on the energy exchange with WBL, relative variations of the WWI parameter, produced by the non-linear mode interaction, are much smaller than the empirical data scatter. Thus, according to Pierson and Moskovitz (1964), the estimations of the parameter $\beta$ differ by a factor of 2-3 for $\omega\sim 1$, and by an order of magnitude for $\omega\sim 0.1$. The same scatter of the WWI parameter values provides various approximate formulas (see Table 3 in Burgers and Makin, 1993 for reference). Moreover, the numerical values of the WWI parameter, obviously, depend on the parameterization scheme for turbulent drag, vertical, and horizontal resolution used in the numerical model, etc.

Summarizing all that has been said, it is possible to conclude that to a first approximation, the mutual influence of the wave components may be neglected. Thus, the superposition principle may be considered to be satisfied, and the function $\beta(\omega)$ obtained using the numerical experiments with airflow over the single-mode surface may be used for calculations of the momentum and energy fluxes.

### 4.3 Arbitrary Wind Direction

The general non-symmetric case of angular wave distribution, with respect to the wind direction, is considered. In terms of the WWI parameter, this means that the symmetry axes of the 2D $\beta(\tilde{\omega},\theta)$ parameter distribution and the spatial wave distribution $D(\tilde{\omega},\theta)$ are directed at an angle $\phi$ with respect to each other. In order to figure out how erroneous the previous assumption ($\phi$=0) is, a number of numerical experiments with the 1D WBL model have been carried out. The model has been modified to take into account an arbitrary angle $\phi$. Namely, the wave- induced momentum flux is now the function of two arguments

$$\tau(\zeta,\phi)=\rho_{wg}\int_0^{\omega_*}F(\omega,\phi)f(\zeta)d\omega \tag{36}$$

where

$$F(\omega,\phi)=\int_{-\pi}^{\pi}kS(\omega)D(\omega,\theta)\beta(\omega,\theta-\phi)d\theta \tag{37}$$

The waveward energy flux $\varepsilon$ is written, respectively

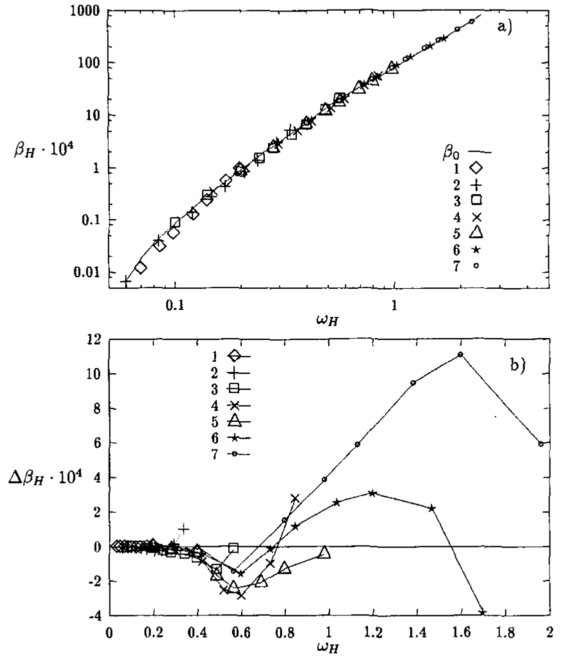


I g. 7 Dependence of the parameter $\beta_H$ (a) and the c fferences $\Delta\beta_H = \beta_H - \beta_0$ (b) on the frequency $w_H$ for \ rious values of the frequency $w_L$ : 1)0.035 ; 2) 0.06 : 3) 0.1 ; 4 0.15 ; 5) 0.5 ; 6) 0.3 ; 7) 0.4

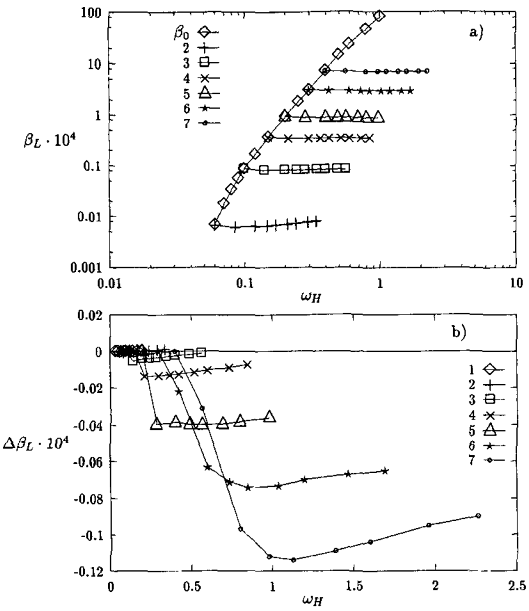


ig. 8 Dependence of the parameter $\beta_L$ (a) and the lifferences $\Delta\beta_L = \beta_L - \beta_0$ (b) on the frequency $w_H$ for 'arious values of the frequency $w_L$ : 1)0.035 ; 2) 0.06 : 3) .1 ; 4) 0.15 ; 5) 0.5 ; 6) 0.3 ; 7) 0.4

$$\varepsilon(\omega,\phi) = \rho_w \int_{-\pi}^{\pi} \omega S(\omega) D(\omega,\theta) \beta(\omega,\theta-\phi) d\theta \qquad (38)$$

Fully developed sea has been described, via the Pierson-Moscovitz spectrum (23). The developing wave situation has been specified by the known 2D model spectrum JONSWAP (25). Since the Pierson-Moscovitz spectrum is one-dimensional, the JONSWAP angular distributions (28) have been considered in this case. The *wind-wave interaction parameter* has been calculated, using the 2D approximate formulas suggested by Chalikov and Belevich (1993), Makin and Mastenbroek (1996), and the WAMDI Group (Zaslavsky et al., 1995). All the approximate formulas for the WWI parameter are written below.

Chalikov-Belevich (Chalikov and Belevich, 1993):

$$\beta(\tilde{\omega},\theta) = 10^{-4}$$

$$\begin{array}{ll} -a_1 \tilde{\omega}_a^{\,2} - a_2, & \tilde{\omega}_a < -1 \\ a_3 \tilde{\omega}_a (a_4 \tilde{\omega}_a - a_5) - a_6, & \tilde{\omega}_a \in (-1, \frac{1}{2}\Omega_1) \\ (a_4 \tilde{\omega}_a - a_5)\tilde{\omega}_a, & \tilde{\omega}_a \in (\frac{1}{2}\Omega_1, \Omega_1) \\ a_7 \tilde{\omega}_a - a_8, & \tilde{\omega}_a \in (\Omega_1, \Omega_2) \\ a_9(\tilde{\omega}_a - 1)^2 + a_{10}, & \tilde{\omega}_a > \Omega_2 \end{array}$$

Here $\tilde{\omega}_a = \tilde{\omega}\frac{u_\lambda}{v_*}\cos\theta$, $u_\lambda$ is the absolute value of the wind speed at the height equal to the "apparent" wave length $\lambda_a = \frac{2\pi v_*^2}{\omega^2 g \cos\theta}$, $a_1, \ldots, a_{10}$ and $\Omega_1$, $\Omega_2$ are parameters which depend on the drag coefficient at height $\zeta = \lambda_a$:

$$\begin{array}{ll} \Omega_1 = 1.075 + 75\,C_\lambda, & \Omega_2 = 1.2 + 300 C_\lambda \\ a_1 = 0.25 + 395\,C_\lambda, & a_3 = (a_0 - a_2 - a_1)/(a_0 + a_4 + a_5) \\ a_2 = 0.35 + 150\,C_\lambda, & a_5 = a4\,\Omega_1 \\ a_4 = 0.30 + 300\,C_\lambda, & a_6 = a_0(1 - a_3) \\ a_9 = 0.35 + 240\,C_\lambda, & a_7 = (a_9(\Omega_2 - 1)^2 + a_{10})/(\Omega_2 - \Omega_1) \\ a_{10} = -0.06 + 470 C_\lambda, & a_8 = a_7 \Omega_1 \\ & a_0 = 0.25 a_5^2 / a_4 \end{array}$$

Makin-Mastenbroek (1996):

$$\beta(\tilde{\omega},\theta) = 16\frac{\rho_a}{\rho_w}\,\omega^2\cos^2\theta$$

WAMDI Group (Zaslavsky et al., 1995):

$$\beta(\tilde{\omega}, \theta) = \max\left\{0.25\frac{\rho_a}{\rho_w}(28\,\tilde{\omega}\cos\theta - 1), 0\right\} \quad (39)$$

Though different approximations for the WWI parameter have been used, the results obtained are quite similar. We illustrate our calculations using the WAM formula (39). The dependence of the drag coefficient $C$ on the angle $\phi$, between the symmetry axes of the wave angular distribution and the 2D WWI parameter, is very weak at any height. The maximum relative change $\delta C$ of $C(\phi)$, with respect to $C(0)$, decreases with growing fetch, and is approximately proportional to the logarithm of the peak frequency $\tilde{\omega}_p$. For example, for the Pierson - Moscovitz spectrum, $\delta C < 0.1\%$. In the case of developing waves (JONSWAP spectrum), our computation results are summarized in Table 1, below.

**Table 1.** Computation results of developing waves

| $\tilde{\omega}_p$ | 0.04 | 0.06 | 0.15 | 0.2 |
|---|---|---|---|---|
| $\delta C$ | $<0.5\%$ | $<2\%$ | $<4\%$ | $<5\%$ |

This unexpected result, however, has a simple explanation. Note that the wave drag is caused mainly by the high- frequency part of the wave spectrum. These HF wave components have small phase velocities in comparison to wind velocity, and act, to a great extent, as roughness elements of the surface, and are indifferent to the wind direction.

This reasoning does not yet explain the above-written dependence $\delta C(\tilde{\omega}_p)$. The decrease of $\delta C$ with growing fetch is determined by the JONSWAP wave spectrum model, which has been used in the current research. As has been mentioned, the specific feature of this spectrum is the overshoot effect, i.e. an increase in the value of the spectral energy density $S_J(\tilde{\omega})$ with the increase of the peak frequency $\tilde{\omega}_p$, for any given frequency $\tilde{\omega} > \tilde{\omega}_p$. Thus, contribution of the HF wave components to the overall drag decreases with growing wave age.

To verify this supposition, we have repeated the last numerical experiments, using another wave spectrum model that, contrary to JONSWAP, does not possess the overshoot feature. Such a spectrum has been suggested by Donelan et al, (1985):

$$S_D(\tilde{\omega}) = \left(\alpha_D\ \tilde{\omega}_p^{-5}\right) o^{-4} \exp\left(-\frac{5}{4} o^{-4}\right) \gamma_D^{G_D} \quad (40)$$

where

$$\alpha_D = 0.042\ \tilde{\omega}_p^{0.55}$$

$$\gamma_D = \begin{cases} 1.7 & \tilde{\omega}_p \le 0.0414 \\ 10. + 6\ \lg\ \tilde{\omega}_p & \tilde{\omega}_p > 0.0414 \end{cases} \quad (41)$$

$$G_D = \exp\left(-\frac{1}{2}\left(\frac{1-o}{\sigma_D}\right)^2\right)$$

$$\sigma_D = 0.08\left(1 + 3 \cdot 10^{-4}\ \tilde{\omega}_p^{-3}\right) \quad (42)$$

The wave angular distribution function is as follows:

$$D_D(\tilde{\omega}, \theta) = \frac{1}{2} q\ \mathrm{sech}^2(q\theta)$$

where

$$q = \begin{cases} 2.61, o^{1.3}, & o \in (0.56, 0.95) \\ 2.28, o^{-1.3}, & o \in (0.95, 1.6) \\ 1.24, & \textit{otherwise} \end{cases}$$

Indeed, the fetch dependence of the $\delta C$ has disappeared with a change of the spectrum model. For the spectrum of Donelan et al, the value of $\delta C$ is approximately 7% for any peak frequency.

Anyway, the error introduced by the assumption of $\phi = 0$ is small, and may be neglected in the parameterization schemes of the wave boundary layer.

## 5. Concluding Remarks

It has been shown that the simplifying assumption of the 1D model of WBL, and the parameterization scheme based on it, cannot introduce big mistakes in the values of the drag and fluxes of momentum and energy on the sea-air interface. All of the chain of the energy transfer from wind to waves and currents has been discussed in Chalikov and Belevich (1993). Here, we can add that for a rough scheme of ocean-atmosphere interaction on the mesoscales in the framework of coupled ocean-atmosphere models can be developed. It may define the drag and fluxes on the ocean-atmosphere interface, directly, from the main meteorological characteristics at the lowest computational (observational) level in the atmosphere. A similar approach has been demonstrated in the works of Zilitinkevich and Chalikov (1968).

## Acknowledgements

This work was supported by a grant No. 2000-2-305-001-2 from Korea Sciece & Engineering Foundation.


## References


Belevich, M. (1996). "On the Influence of Thermal Stratification on the Structure of the Wave Boundary Layer," Izv. Atmos. Ocean. Phys., Vol 32, pp 397-401 (in Russian).

Belevich, M. and Neelov, I. (1998). "On the Approximation of the Wind-Wave Interaction Parameter," Izv. Atmos. Ocean. Phys., Vol 34, pp 435-440 (in Russian).

Belevich, M. and Neelov, I. (2000). "Evaluation of the Mutual Influence of the Wind-Wave Components on the Energy Interchange with the Wave Boundary Layer," Meteorologiya i Gidrologiya, No 1, pp 70-78 (in Russian).

Burgers, G. and Makin, V. (1993). "Boundary-Layer Model Results for Wind-Sea Growth," J. Phys. Oceanogr., Vol 23, pp 372-385.

Chalikov, D. and Belevich, M. (1993). "One-dimensional Theory of the Wave Boundary Layer," Bound. Layer Meteorol., Vol 63, pp 65-96.

Donelan, M.A., Hamilton, J. and Hui, W.H. (1985). "Directional Spectra of Wind-Generated Waves," Phil. Trans. Roy. Soc. London, Vol A315, pp 509-562.

Hasselmann, K., Barnett, T.P., Bouws, E., Carlson, H., Cartwright, D.E., Enke, K., Ewing, J.A., Gienapp, H., Hasselmann, D.E., Kruseman, P., Meerburg, P., Muller, Olbers, D.J., Richter, K., Sell, W. and Walden. H. (1973). "Measurements of Wind-Wave Growth and Swell Decay During the Joint Sea Wave Project (JONSWAP)," Dtsch. Hydr. Z., Bd. A8 (12), pp 1-95.

Hasselmann, D.E., Dunckel, M. and Ewing. J.A. (1973). "Directional Wave Spectra Observed During JONSWAP," J. Phys. Oceanogr., Vol 10, pp 1264-1280.

Makin, V.K. (1983). "On the Wind Energy Transfer to Surface Gravity Waves," Okeanologiya, Vol XXIII, pp 569-574 (in Russian).

Makin, V. and Chalikov, D. (1983). "Calculation of Momentum and Energy Fluxes going to Developing Waves," Izv. Atmos. Ocean. Phys., Vol 22, pp 1015-1019 (in Russian).

Makin, V.K. and Mastenbroek, C. (1996). "Impact of Waves on Air-Sea Exchange of Sensible Heat and Momentum," Bound. Layer Meteorol., Vol 79, pp 279-300.

Monin A.S. and Yaglom, A.M. (1971). Statistical Fluid Mechanics, Vol 1, MIT Press, Cambridge.

Pierson, W.J. and Moskovitz, L. (1964). "A Proposed Spectral Form for Fully-Developed Wind Seas Based on the Similarity Theory of S.A. Kitaigorodskii," J. Geophys. Res., Vol 69, No 24, pp 5181-5190.

Plant, W.J., Relationship, A. (1982). "Between Wind Stress and Wave Slope," J. Geophys. Res., Vol 87, pp 1961-1967.

WAMD Group (Hasselmann, S., Greenwood, J.A., Reistad, M., Zambresky, L., and Ewing, J.A.) (1988). "The WAM Model - A Third Generation Ocean Wave Prediction Model," J. Phys. Oceanogr., Vol 18, pp 1775-1810.

Zaslavsky, M.M., Kabatchenko, I.M., and Matushevsky, G.V. (1995). "Joint Adaptive Model of the Nearwater Wind and Wind Waves," In Davidan, I.N. (ed.) Research Problems and Mathematical Modeling of the Wind Waves, Gidrometeoizdat, St. Petersburg (in Russian).

Zilitinkevich, S.S. and Chalikov, D.V. (1968). "Determination of Universal Profiles of Wind and Temperature in the Near-Earth Atmospheric Layer," Izv. Atmos. Ocean. Phys., Vol 4, pp 294-302 (in Russian).